

## Swept laser source at 1 $\mu\text{m}$ for Fourier domain optical coherence tomography

Jun Zhang,<sup>a)</sup> Qiang Wang, Bin Rao, and Zhongping Chen<sup>b)</sup>

Beckman Laser Institute, University of California, Irvine, Irvine, California 92612 and Department of Biomedical Engineering, University of California, Irvine, Irvine, California 92612

Kevin Hsu

Micron Optics Inc., 1852 Century Place Northeast, Atlanta, Georgia 30345

(Received 9 May 2006; accepted 21 June 2006; published online 16 August 2006)

A frequency swept source at 1  $\mu\text{m}$  wavelength for Fourier domain optical coherence tomography (FDOCT) was demonstrated. The source incorporates a fiber-coupled semiconductor optical amplifier gain module, a fiber Fabry-Pérot tunable filter, and fiber isolators to form a ring laser. The laser is capable of a scanning range of 64 nm, 3 dB sweep range of 31 nm, and coherence length of 9.8 mm at 2 kHz sweep rate. Based on the swept source, a FDOCT system was developed which can achieve 12  $\mu\text{m}$  axial resolution in tissue. Imaging of pig retina was demonstrated with the FDOCT system. © 2006 American Institute of Physics. [DOI: 10.1063/1.2335405]

Optical coherence tomography (OCT) is a noninvasive, noncontact imaging modality that uses coherent gating to obtain high-resolution, cross-sectional images of tissue microstructure.<sup>1</sup> OCT has been especially powerful for ophthalmic imaging where it can provide images of retinal pathology with unprecedented resolutions.<sup>2,3</sup> Current OCT systems for ophthalmic applications use light sources centered at 0.8  $\mu\text{m}$ . Although high-resolution OCT at 0.8  $\mu\text{m}$  provides a clear image of the intraretinal layer, its penetration depth is not enough for imaging the choroid beyond the retina.<sup>4</sup> Increasing center wavelengths longer than 0.8  $\mu\text{m}$  should increase imaging depth due to reduced scattering at longer wavelengths. However, water absorption also increases at longer wavelengths. A center wavelength at 1  $\mu\text{m}$  provides an optimal wavelength for imaging choroidal morphology and microvasculature below the retinal pigment epithelium.<sup>4</sup> It was also shown that tissue dispersion is minimal in that wavelength range.<sup>5</sup> In addition, eye-safe exposure at 1  $\mu\text{m}$  is a factor of 3.3 larger than that at 0.8  $\mu\text{m}$ , which permits the use of a higher incident power for ocular imaging.<sup>6</sup> Therefore, with deeper penetration and improved sensitivity, OCT imaging near the 1  $\mu\text{m}$  wavelength could be more beneficial than near 0.8  $\mu\text{m}$ .

Fourier domain OCT (FDOCT) measures interference fringes in the spectral domain to reconstruct a tomographic image. Modulation of the interference fringe intensity in the spectral domain is used to determine the location of all scattering objects along the beam propagation direction. FDOCT offers significantly improved sensitivity and imaging speed compared to time domain OCT.<sup>7-15</sup> Two methods have been developed to employ the Fourier domain technique: FDOCT using a spectrometer with a line-scan camera<sup>7-9</sup> and FDOCT using a rapidly swept laser source, i.e., “swept source OCT” (SSOCT).<sup>10-15</sup> SSOCT has the advantage of a simple system setup, low cost, and capability of balanced detection. In addition, mirror image and autocorrelation noise can be removed instantaneously by the simple addition of an electro-optic modulator.<sup>12</sup> However, at the center wavelength of

1  $\mu\text{m}$ , there is currently no swept source appropriate for FDOCT. In this letter, we report the development of a frequency swept source centered at 1060 nm for the FDOCT system. With the FDOCT system based on this swept source, high speed imaging of the retina with 12  $\mu\text{m}$  axial resolution was demonstrated.

The 1  $\mu\text{m}$  swept source configuration is illustrated in Fig. 1. The source design incorporates a semiconductor optical amplifier (SOA) gain module, a fiber Fabry-Pérot tunable filter (FFP-TF), two double-stage isolators, and a fiber coupler to form a unidirectional ring laser of 2.5 m cavity length. The SOA driven at 400 mA current bias provides a small signal gain of  $\sim 18$  dB at the center wavelength and a gain bandwidth of  $\sim 68$  nm. The FFP-TF controlled by a piezoelectric transducer was used for the critical wavelength tuning operation. The FFP-TF has a free spectral range of  $\sim 110$  nm, a bandwidth of  $\sim 0.055$  nm, and a loss of  $\sim 1$  dB. The two isolators with a typical loss of 2.5 dB each are required to force unidirectional propagation in the ring cavity. By including the 10% output coupling and some splice losses, the resultant total cavity loss is  $\sim 7$  dB. At the laser

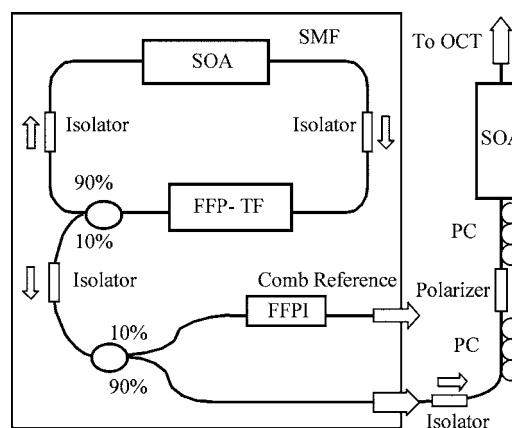


FIG. 1. Schematic of the 1  $\mu\text{m}$  swept laser source. Wavelength tuning is performed by the fiber Fabry-Pérot tunable filter (FFP-TF). A small portion of the laser output is fed to a fiber Fabry-Pérot interferometer (FFPI) to generate a comb reference. SMF, single-mode fiber; SOA, semiconductor optical amplifier; PC, polarization controller.

<sup>a)</sup>Electronic mail: junzhang@uci.edu

<sup>b)</sup>Electronic mail: z2chen@uci.edu

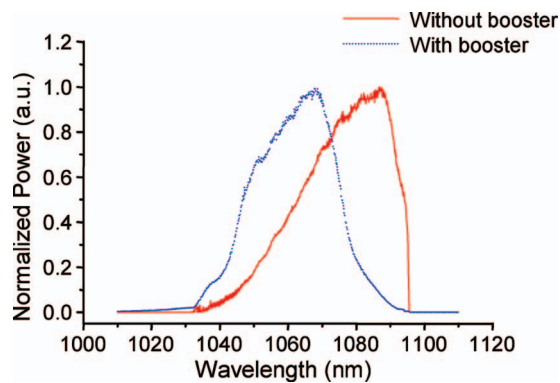


FIG. 2. (Color) Spectra of the swept source without (red curve) and with (blue curve) booster amplifier at a sweep rate of 2 kHz.

output, 10% of the light was split and propagated through an incorporated fiber Fabry-Pérot interferometer (FFPI) that exhibits a uniformly spaced resonance frequency comb of 27 GHz for calibration of the swept wave number function. To increase the power level, the output light was amplified by another SOA acting as a booster amplifier. A polarizer and two static polarization controllers were used to adjust the polarization state of the polarized output light to obtain maximum gain in the polarization dependent booster SOA. At a scanning rate of 2 kHz, the peak power from the laser can be amplified from 0.7 to 4 mW.

The output spectra of the laser measured with an optical spectrum analyzer are shown in Fig. 2. The laser without the booster amplifier is capable of a scanning range of 64 nm (1032–1096 nm) and a full width at half maximum (FWHM) sweep bandwidth of 31 nm centered at 1078 nm (red curve). It was demonstrated that the application of a booster with a blueshifted gain spectrum can partly compensate for the asymmetric shape of the swept spectrum which is due to the nonlinear frequency downshifting mechanism in the laser gain medium.<sup>11</sup> By choosing an appropriate booster gain spectrum, the asymmetric spectrum was partly shaped (blue curve, Fig. 2). The center wavelength was shifted to 1061 nm while the FWHM sweep bandwidth and scanning range were kept the same. In FDOCT, the imaging depth is determined by the instantaneous linewidth of the swept laser source which can be calculated by measuring the coherence length with a variable-delay Michelson interferometer.<sup>16</sup> From the decayed fringe visibility with increased optical path length delays, the coherence length of the swept source amplified by the booster SOA was determined to be 9.8 mm corresponding to the instantaneous linewidth of 0.05 nm.

The schematic diagram of the FDOCT system based on the built swept source is shown in Fig. 3. The source was driven by a 2 kHz sinusoidal signal. To increase the signal-to-noise ratio of the system, a balanced detection configuration was constructed by use of two 50/50 fiber couplers.<sup>17</sup> The output light from the swept source was split into reference and sample arms by a 2×2 coupler. In the reference arm, an adjustable neutral density attenuator was used to attenuate the reference power for enhanced sensitivity. In the detection arm, the signal from the balanced detector was converted by a data acquisition board sampling at 10 MHz. The number of data points for each A-line data acquisition during the frequency scan was 1024. The detected fringe signal was transformed from time to wave number space with the swept spectra function which was determined with the uniformly

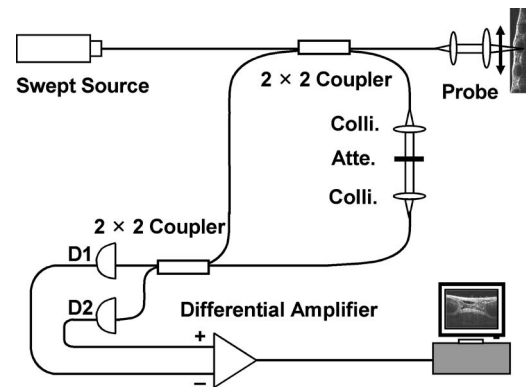


FIG. 3. Schematic of the FDOCT system: Colli., collimator; Atte., adjustable neutral density attenuator; D1 and D2, photodetectors.

spaced frequency signal from the comb reference port of the laser.<sup>11,12</sup> Dispersion should be compensated since dispersion mismatch in sample and reference arms would broaden the coherence function and thus degrade the axial resolution of the system. In our FDOCT system, dispersion compensation was fulfilled by calibrating the nonlinear phase function in wave number space with a sample reflector. The consequent fast Fourier transform performed in wave number space retrieved the complex depth encoded signal.

From the amplitude information of the complex signal, the structure image can be acquired. By measuring the point spread function with a partial reflector at a depth of 900  $\mu\text{m}$  in the sample arm, the axial resolution in free space was determined to be 17  $\mu\text{m}$  corresponding to the effective axial resolution of 12  $\mu\text{m}$  in tissue. The measured axial resolution in free space is very close to the theoretical resolution of 16  $\mu\text{m}$  determined by the FWHM sweep bandwidth of the swept source.

To illustrate the performance of the system in biological, especially ophthalmic, tissues, *in vitro* pig retina was im-

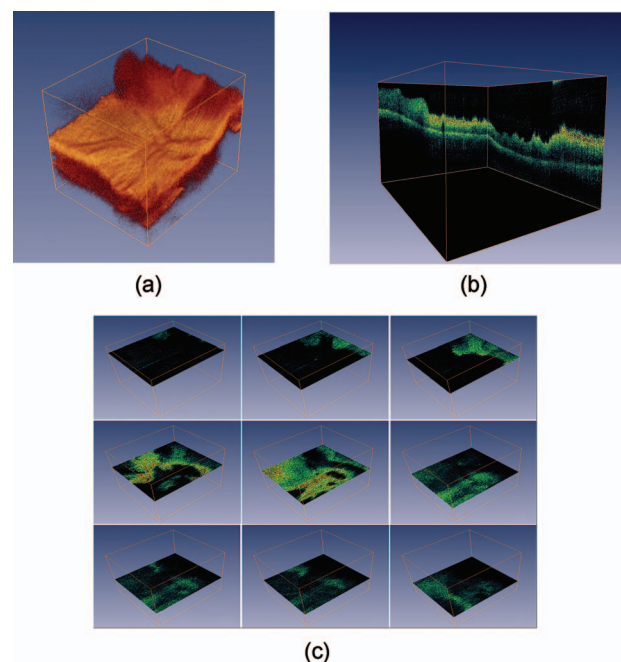


FIG. 4. (Color) (a) 3D imaging of pig retina with FDOCT system. (b) 2D cross-sectional images by slicing the image in the  $x$ ,  $y$ , and  $z$  directions. (c) 2D images sliced at different depths.

aged. The fresh excised pig eye was preserved in formalin. The three dimensional (3D) imaging of pig retina obtained with the FDOCT system is shown in Fig. 4. The 3D image occupies a volume of  $5 \times 3.3 \times 2.9 \text{ mm}^3$ . The two dimensional (2D) imaging is reconstructed at the rate of 4 frames/s. The 3D image is obtained by combining 290 2D images. With 3D volume data, 2D slice images can be reconstructed in any direction by slicing the 3D image as shown in Figs. 4(b) and 4(c).

In summary, a swept source at  $1 \mu\text{m}$  wavelength for FDOCT was developed. The laser is capable of 3 dB sweep range of 31 nm and a coherence length of 9.8 mm at 2 kHz sweep rate. The swept source based FDOCT system can achieve  $12 \mu\text{m}$  axial resolution in tissue. With the FDOCT system, three dimensional imaging of pig retina was demonstrated.

This work was supported by research grants from the National Science Foundation (BES-86924), National Institute of Health (EB-00293, NCI-91717, and RR-01192), Air Force Office of Scientific Research (FA9550-04-1-0101), and the Beckman Laser Institute Endowment.

<sup>1</sup>D. Huang, E. A. Swanson, C. P. Lin, J. S. Schuman, W. G. Stinson, W. Chang, M. R. Hee, T. Flotte, K. Gregory, C. A. Puliafito, and J. G. Fujimoto, *Science* **254**, 1178 (1991).

<sup>2</sup>W. Drexler, U. Morgner, R. K. Ghanta, F. X. Kärtner, J. S. Schuman, and

J. G. Fujimoto, *Nat. Med.* **7**, 502 (2001).

<sup>3</sup>W. Drexler, H. Sattmann, B. Hermann, T. H. Ko, M. Stur, A. Unterhuber, C. Scholda, O. Findl, M. Wirtitsch, J. G. Fujimoto, and A. F. Fercher, *Arch. Ophthalmol. (Chicago)* **121**, 695 (2003).

<sup>4</sup>A. Unterhuber, B. Povazay, B. Hermann, H. Sattmann, A. Chavez-Pirson, and W. Drexler, *Opt. Express* **13**, 3252 (2005).

<sup>5</sup>Y. Wang, J. Nelson, Z. Chen, B. Reiser, R. Chuck, and R. Windeler, *Opt. Express* **11**, 1411 (2003).

<sup>6</sup>American National Standards Institute, American National Standard for Safe Use of Lasers, Standard z136.1 (ANSI, Orlando, FL, 2000).

<sup>7</sup>G. Hausler and M. W. Lindner, *J. Biomed. Opt.* **3**, 21 (1998).

<sup>8</sup>R. A. Leitgeb, C. K. Hitzenberger, and A. F. Fercher, *Opt. Express* **11**, 889 (2003).

<sup>9</sup>Y. Zhang, B. Cense, J. Rha, R. S. Jonnal, W. Gao, R. J. Zawadzki, J. S. Werner, S. Jones, S. Olivier, and D. T. Miller, *Opt. Express* **14**, 4380 (2006).

<sup>10</sup>S. H. Yun, G. J. Tearney, J. F. de Boer, N. Iftimia, and B. E. Bouma, *Opt. Express* **11**, 2953 (2003).

<sup>11</sup>R. Huber, M. Wojtkowski, K. Taira, J. G. Fujimoto, and K. Hsu, *Opt. Express* **13**, 3513 (2005).

<sup>12</sup>J. Zhang, J. S. Nelson, and Z. Chen, *Opt. Lett.* **30**, 147 (2005).

<sup>13</sup>Y. Yasuno, V. Madjarova, S. Makita, M. Akiba, A. Morosawa, C. Chong, T. Sakai, K. Chan, M. Itoh, and T. Yatagai, *Opt. Express* **13**, 10652 (2005).

<sup>14</sup>Anjul M. Davis, Michael A. Choma, and Joseph A. Izatt, *J. Biomed. Opt.* **10**, 064005 (2005).

<sup>15</sup>R. Huber, M. Wojtkowski, and J. G. Fujimoto, *Opt. Express* **14**, 3225 (2006).

<sup>16</sup>S. H. Yun, C. Boudoux, M. C. Pierce, J. F. de Boer, G. J. Tearney, and B. E. Bouma, *IEEE Photonics Technol. Lett.* **16**, 293 (2004).

<sup>17</sup>A. Podoleanu, *Appl. Opt.* **39**, 173 (2000).